

A dielectric theory for the coupling of light with multiple inter-subband transitions

T. SCHMIELAU, M. F. PEREIRA*

Materials and Engineering Research Institute, Sheffield Hallam University, Howard Street, Sheffield, S1 1WB, Great Britain

This paper studies the coupling of light with intersubband excitations in the case of multiple transitions. It is used a realistic input from a nonequilibrium many body solver in order to describe a microresonator with an active core region based on a successful quantum cascade laser design.

(Received June 5, 2007; accepted January 7, 2008)

Keywords: Many-body theory, Quantum cascade lasers, Inter-subband transitions, Non-equilibrium distribution functions, Inter-sub-band antipolariton

1. Introduction

The microcavity polarity splitting of inter-subband transitions has been predicted theoretically [1] and observed experimentally [2, 3]. However, a recent publication has demonstrated that the coupling between light and intersubband excitations in semiconductors is fundamentally different from the well understood coupling to interband transitions that leads to excitonic polaritons and a more appropriate “inter-subband antipolariton” concept has been introduced [4]. This microscopic Keldysh Green’s functions formalism leads to analytical expressions for the quasi-particle dispersion including many body effects under non-equilibrium conditions. It consistently reproduces dispersion relations found experimentally if light is absorbed due to inter-subband transitions [2, 3] and lead to unique features not previously found in the literature, namely (i) Anomalous dispersions under population inversion conditions that cannot be described a Hamiltonian theory based on bosonic approximations were predicted. (ii) The limit of validity of the conventional polariton as a bosonic quasiparticle concept has been demonstrated numerically for the inter-sub-band case and a simple recipe to control bosonic effects and turn them on and off by selective excitation of the subbands has been given.

(iii) The influence of the dominating many body corrections on the dispersion of both passive (absorption) and active (inverted gain media) has been discussed. In Ref. [4] only one resonance has been considered. The multiple resonance case requires a numerical solution of the dispersion relation equations and is the main topic of the present manuscript,

2. Mathematical formulas

The microcavity mode is determined by the wave equation

$$\Delta E(\omega) + \frac{\omega^2}{c^2} \varepsilon(\omega) E(\omega) = 0 \quad (1)$$

If the imaginary part of the dielectric function is neglected with respect to the real part, the simple Ansatz solution can be used

$$E(\omega) = E_0 e^{ik_x x} \sin \frac{\pi z}{L_c} \quad (2)$$

describing to quantization of the optical modes in a microcavity of length L_c . Snell’s law imposes the conservation of $k_x = \omega/c n_s \sin \theta = \dots = \omega/c n_b \sin \theta_b$, where n_b and θ_b are respectively the effective refractive index and the angle of refraction inside the cavity. θ is the angle of incidence from the substrate with refractive index n_s as shown in Fig. 1 The structure follows those described in recent literature, [2, 3] but a different active core region is used here. Quasi-particle dispersions can be derived and more clearly explained by means of an effective medium approach that leads to simple analytical formulae for multilayers. The cavity core effective dielectric function is given by

$$\varepsilon_b = (L_c)^{-1} \sum_{j=1}^N L_j \cdot \varepsilon_j \quad (3)$$

where L_j and ε_j denote respectively the widths and background dielectric constants of the alternating barrier and well layers in the cavity core, plus a cap GaAs layer to avoid oxidation due to the Al content of the barriers. The cavity length is simply $L_c = \sum_{j=1}^N L_j$ for a total of N layers. In recent experiments [2, 3], the energy positions of the dips in reflectance spectra have been adjusted to a

phenomenological formula yielding the inter-subbandpolariton dispersion as a function of incidence angle. In the dielectric approach presented here, the quasi-particle dispersion relations, or in other words, the energy $\hbar\omega$ as a function of wave number k_x (or the incidence angle θ) are directly obtained by mapping the roots of the secular equation,

$$k_x^2 + \frac{\pi^2}{L_c^2} = \frac{\omega^2}{c^2} \varepsilon(\omega) \quad (4)$$

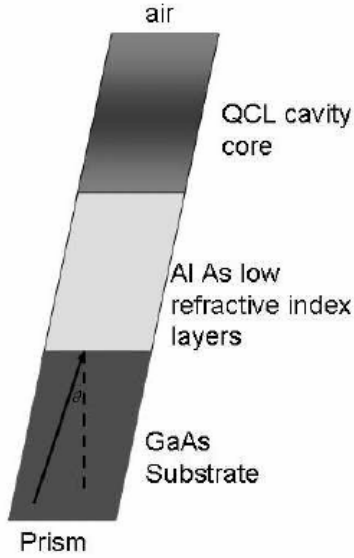


Fig. 1. Diagram indicating the microcavity geometry considered. Light reflected at the bottom of the GaAs substrate reaches the AlAs layers within incidence angle θ . The light is confined through internal reflection at the sample surface (interface with air) in one side and in the other side at the interface with the low index AlAs layer. The dispersions in the next figure are given as a function of θ following the convention used in recent experiments [2, 3].

where c is the speed of light in vacuum. The optical susceptibility yields the connection between the macroscopic dielectric constant and the microscopic resonances in the medium. In the frequency domain, the relation reads

$$\varepsilon(\omega) = \varepsilon_b [1 + 4\pi\lambda\chi(\omega)] \quad (5)$$

where ε_b is the background dielectric constant, and $\lambda = N_w L_w / L_c$ where N_w and L_w denote respectively the number of quantum wells and the well width, consistently with Eq. 3.

The optical susceptibility due to presence of carriers in a single well is given by

$$\chi(\omega) = 2 \sum_{\mu \neq \nu, k} \wp_{\mu\nu} \chi_{\nu, \mu}(k, \omega) \quad (6)$$

where $\wp_{\mu\nu} = e d_{\mu\nu} \sin\theta_b$ is the projected transition dipole moment between subbands ν and μ , which are labelled $\nu = 1, 2, \dots$ with increasing energy and by running over all subband indices $\nu \neq \mu$ in Eq. (6), the rotating wave approximation is not used. The susceptibility function $\chi_{\nu\mu}(k, \omega)$ is related to the carriers Keldysh Green's Function G , whose time evolution is described by a Dyson equation. The resulting integro-differential equation for $\chi_{\nu\mu}(k, \omega)$ can be solved numerically including many body effects, complex non parabolic band structure, correlation and dephasing mechanisms. [5-7] Here only the main resulting equations are shown in the Hartree-Fock regime,

$$\begin{aligned} & \hbar\omega - e_{\nu\mu}(k) + i\Gamma_{\nu\mu} \chi_{\nu\mu}(k, \omega) - \\ & - \delta n_{\nu\mu k} \sum_{k' \neq k} \chi_{\nu\mu}(k', \omega) \tilde{V}_{k-k'}^{\nu\mu} = \wp_{\nu\mu} \delta n_{\nu\mu k} \end{aligned} \quad (7)$$

where $\tilde{V}_{k-k'}^{\nu\mu} = V_{k-k'}^{(\nu\nu\mu\mu)} - 2V_{k-k'}^{(\nu\mu\mu\nu)}$.

The population difference is given by $\delta n_{\nu\mu}(k) = n_\nu(k) - n_\mu(k)$. The bare Coulomb interaction matrix elements read

$$V_{k-k'}^{(\mu\nu\beta\alpha)} = \int dz dz' \phi_\mu^*(z) \phi_\nu(z) \frac{2\pi e^2 \exp(-|k-k'|z-z'|)}{\varepsilon|k-k'|} \phi_\alpha^*(z') \phi_\beta(z') \quad (8)$$

and ε_0 denotes the background dielectric constant and the \mathcal{O} 's are the quantum well envelope wave functions. The energy difference between the levels, renormalized by the inter-subband shift is given by

$$\begin{aligned} e_{\nu\mu}(k) = & E_\nu(k) - E_\mu(k) - \sum_{k'} f_\nu(k') V_{k-k'}^{(\nu\nu\nu\nu)} + \\ & + \sum_{k'} n_\mu(k') V_{k-k'}^{(\mu\mu\mu\mu)} + \sum_{k'} [n_\nu(k') - n_\mu(k')] V_{k-k'}^{(\nu\mu\mu\nu)} \end{aligned} \quad (9)$$

The main Many-body corrections at Hartree-Fock level are the exchange term (that leads to excitons for interband transitions), the inter-subband shift and the depolarization. Previous studies demonstrate that the inter-subband shift and exchange corrections largely compensate each other in many cases, and the Coulomb corrections are dominated by the depolarization. [5-7]. Thus, if only the depolarization is kept and parabolic conduction bands with the same effective mass per subband are used, an analytical expression for the optical susceptibility is found

$$\chi(\omega) = - \sum_{\mu \neq \nu} \frac{\Delta_{\mu\nu}}{\hbar\omega - \Delta E_{\nu\mu} - \delta\mathcal{E}_{\nu\mu} + i\Gamma_{\nu\mu}} \quad (10)$$

Here $\Gamma_{\mu\nu}$ is the calculated dephasing, and the longitudinal-transverse splitting reads

$$\Delta_{\mu\nu} = \frac{4\pi}{L\omega} \left| \mathbf{e} \cdot \mathbf{d}_{\mu\nu} \right|^2 \delta n_{\mu\nu} \sin^2 \theta_b \quad (11)$$

where e is the electron charge and $\Delta E_{\nu\mu} = E_\nu - E_\mu$. For a given sample surface S , $\Delta N_{\mu\nu}/S = \delta n_{\mu\nu} = n_\mu - n_\nu$ denotes the intersubband population density differences. The depolarization shift can be expressed as

$$\delta \epsilon_{\nu\mu} = \delta N_{\mu\nu} V \left(\begin{smallmatrix} \nu & \mu \\ 0 & \mu\nu \end{smallmatrix} \right) \equiv \frac{20e^2}{9\pi\epsilon_0} \delta n_{\mu\nu} L_{\mu\nu}^{\text{dep}}$$

Neglecting the dephasing $\Gamma_{\nu\mu}$, an application to the cavity in Fig. 1 is given next.

3. Numerical results and discussion

The numerical results shown next were obtained by starting with a structure similar to those studied in Refs. [2-4] but replacing the isolated quantum well active core region by a qcl structure similar to the very successful mid-infrared design introduced in Ref. [8]. The input for the calculations presented were extracted from Ref. [8] where the non-equilibrium occupations have been evaluated.

Only the main transitions have been considered. The dipole moment, energy levels and nonequilibrium subband occupations are obtained from the solutions of Dyson equations for the nonequilibrium many body Keldysh Green's functions and the resulting input parameters have been extracted from Ref. [4]. In the multiple inter-subband transition case, the longitudinal eigenmodes of the dielectric medium are not simply located at $\hbar\omega_L = \Delta E_{\nu\mu} + \Delta_{\mu\nu}$, because the different resonances interact giving rise to a more complex and interesting scenario than the single resonance case discussed in Ref. [4].

Table 1. Transition parameters. (ν, μ) denotes the lower and higher subbands in a transition, $n_\nu - n_\mu$ is the difference in subband population in units of $10^{11}/\text{cm}^2$. $L_{\nu\mu}^{\text{dep}}$ is the depolarization length in nm.

$E_\mu - E_\nu$ is the energy difference in meV at $k = 0$ including the static mean-field corrections, but no further Coulomb effects. Data taken from [6].

(ν, μ)	$L_{\nu\mu}^{\text{dep}}$	$n_\nu - n_\mu$	$E_\mu - E_\nu$
(6,7)	25.8	2.44	13.3
(7,10)	20.5	1.33	24.2

In summary, the multi inter-subband transition case studied here for a microcavity including a quantum cascade core region shows an interesting interaction between the dispersion branches. The authors hope that

these results will stimulate further experimental studies of light-intersubband coupling in semiconductor heterostructures.

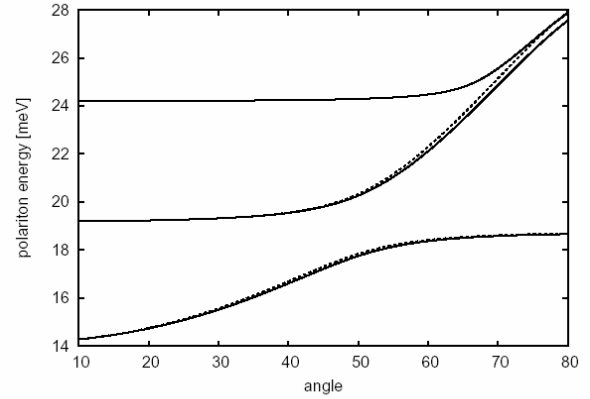


Fig. 2. Intersubband antipolariton dispersions for the two most relevant absorption transitions in a $13.3 \mu\text{m}$ resonator with a structure as depicted in Fig. 1 and a core similar to the quantum cascade laser of Ref. [8] polarized with a bias of 0.12 V/period . The dashed lines were calculated assuming only the lowest transition for comparison.

Acknowledgements

This work was partly supported by the Software Factory Program of Sheffield Hallam University.

References

- [1] A. Liu, Phys. Rev. **B55**, 7101 (1997).
- [2] D. Dini, R. Koehler, A. Tredicucci, G. Biasiol, L. Sorba, Phys. Rev. Lett. **90**, 116401 (2003).
- [3] A. A. Anappara, A. Tredicucci, G. Biasiol, L. Sorba, Appl. Phys. Lett. **87**, 051105 (2005).
- [4] M. F. Pereira, Phys. Rev. **B75**, 195301 (2007).
- [5] M. F. Pereira Jr., H. Wenzel, Phys. Rev. **B70**, 205331 (2004).
- [6] M. F. Pereira Jr., S.-C. Lee, A. Wacker, Phys. Rev. **B69**, 205310 (2004).
- [7] M. F. Pereira Jr., H. Wenzel, Microelectron. Enginering **81**, 510 (2005).
- [8] M. Giehler, R. Hey, H. Kostial, S. Cronenberg, L. Schrottke, H. T. Grahn, Appl. Phys. Lett. **82**, 671 (2003).

*Corresponding author: M.Pereira@shu.ac.uk